Effect of Annealing Temperature on the Structure and Optical Properties of ZnO Nanoparticles for Possible Anti-Bacterial Applications

M. RAI[1], K. KASHYAP[1], A. KHURANA[1], R. VAISAKH[1], S. KUMAR[1], S. KUMAR[1], Y. ARORA[1], A. DHANKHAR[2], CHATTERPAL[2], A. K. DHILLON[2], S. DUDEJA[2] AND A. B. BHATTACHERJEE[3]

[1]Department of Physics, A.R.S.D College, University of Delhi, New Delhi-110021, India
[2]Department of Chemistry, A.R.S.D College, University of Delhi, New Delhi-110021, India
[3]School of Physical Sciences, Jawaharlal Nehru University, New Delhi-110067, India
Corresponding Author Email: aranyabhuti@gmail.com

Abstract

ZnO nanoparticles have been successfully prepared by chemical precipitation method at 200°C, 400°C, 600°C and 800°C. The micro-structure and optical properties of the resulting ZnO nano-particles were investigated by X-ray diffraction (XRD), UV-Visible spectroscopy, Photoluminescence and TEM. ZnO nanoparticles became more crystalline and the average size increases with increasing temperature. The quantum size effect decreases with increase in temperature, since the particle size increases. Quantum confinement increases the band gap energy of ZnO. As temperature increases, the peak absorbance wavelength becomes red shifted due to decreasing quantum confinement with increasing particle size. After high temperature annealing, the usual band edge emission in the UV band (355nm) and the deep level emission in the green band (499 nm) can be seen. TEM data also supports the XRD and optical spectroscopy data.

Keywords: ZnO nanoparticles, micro-structure, optical properties, quantum size effect

Inroduction

In recent years, there has been a significant growth in the development of noble metal oxide nanoparticles due to their unique electrical, optical, chemical and biological properties[1-8]. Among various semiconducting materials, zinc oxide (ZnO) has drawn much attention due to its wide band gap energy of 3.37 eV, high electron mobility of about 2000 cm^2 /(V.s) at 80K [9], large exciton binding energy of 60 meV [10,11] and antibacterial activity [12]. These properties make ZnO a suitable candidate for optoelectronic applications, information storage and sensors [13]. ZnO nanoparticles are also potential candidates for biosensors [14], photodetectors [15] and photocatalysts [16]. Recently, there have been many new routes for the synthesis of ZnO nanoparticles such as organo-metallic precursor method [17], sol-gel synthesis[18], sol-gel combustion[19], zinc-air cell system method[20], precipitation method[21], micro-emulsion route[22]. In this study, chemical precipitation method was used to synthesize ZnO nano-particles. The influence of annealing temperatures on Zn) nano-particles have been reported in some earlier studies [19, 20,23-27]. The primary aim of this investigation is to evaluate the influence of annealing temperature on the size and optical properties of ZnO nano-particles for possible anti-bacterial applications. The micro-structure and optical properties of the resulting ZnO nano-particles were investigated by X-ray diffraction (XRD), UV-Visible spectroscopy, Photoluminescence and TEM.

Materials and Methods

Synthesis And Characterization Of Zno Nanoparticles

The synthesis of ZnO nano-particles were carried out by chemical-precipitation method. All the chemical reagents were of analytical grade which were used in the experiments without further purification and treatment. The procedure adopted to synthesize ZnO nano-particles are as follows: $ZnCl_2$ and $NH_4\ HCO_3$ solutions were prepared according to the desired molar ratio. Stoichiometric dodecyl sodium sulfate (SDS) solution was added into the solution of $NH_4\ HCO_3$. Under constant magnetic stirring, the solution of $ZnCl_2$ was added drop wise in the solution of $NH_4\ HCO_3$ + SDS. After 2 hours, the product was filtered and washed with anhydrous ethanol followed by drying for 4 hours at 50^0 C. Finally, the ZnO nano-particles of different sizes were obtained after annealing in air under different temperatures for 1 hour in the furnace chamber. The structure of ZnO nanoparticles were determined using X-Ray powder diffraction (Rigaku-Miniflex-600) with CuK_α radiation of 1.54059 Å wavelength. The optical characterization of the sample was recorded on UV-visible absorption Spectrophotometer (Shimatzo's UV visible spectrophotometer-1800). The photoluminescence (PL) spectrum of the ZnO nanoparticles has been measured using a spectrofluorimeter (F-2500 FL Spectrophotmeter, Hitachi). The morphology of the ZnO nanoparticles was examined with the help of Jeol 2100F TEM machine.

Results and Discussions:

X-Ray Diffraction Analysis (Xrd)

The XRD patterns of the samples formed under different temperatures are shown in Figure 1. The diffraction peaks at scattering angle (2θ) of 31.8˚, 34.5 ˚, 36.3 ˚, 47.6 ˚ , 56.6 ˚ , 62.7 ˚ , 66.3˚ , 67.9˚ , 69.1˚ correspond to the reflections from (100), (002), (101), (102), (110), (103), (200), (112) and (200) crystal planes respectively. All the diffraction peaks can be well indexed as the hexagonal Wurtzite ZnO phase. Since no excess peaks were formed, it indicates that there were no impurities in the samples. As the annealing temperature increased, the diffraction peaks became narrower and exhibited a higher intensity which demonstrates that the ZnO nanoparticles became more crystalline with increasing temperature. Narrowing of the peak with increasing temperatures suggests that the average size of the nanoparticles became bigger.

According to the XRD data, we observe an increase in the peak intensities as the temperature increases for the diffraction peaks of (100), (002), (101), (102), (110) and (103) planes. The Wurtzite structure of bulk ZnO nanoparticles have unit cell parameters, $a_0 = b_0 = 3.253$ Å and $c_0 = 5.2066$ Å while for ZnO polycrystalline powder is $a_0 = b_0 = 3.249$ Å and $c_0 = 5.21$ Å. These are in agreement with JPCDS card no. 36-1451. The lattice parameters of ZnO nanoparticles annealed at different temperatures were calculated using Miller indices {hkl} according to the equation,

$$\left(\frac{1}{d_{hkl}}\right)^2 = \frac{4/3\,(h^2 + k^2 + hk)}{a^2} + \frac{l^2}{c^2} \qquad (1)$$

Using the diffraction peaks corresponding to the (100) and (002) planes, the lattice constants are displayed in table 1 at various temperatures. At T= 250˚ C, the c-parameter and the a-parameter values are close to that of polycrystalline state while at T = 800˚ C, it is approaching the bulk value. This change in lattice parameters can be attributed to the change in particle size and quantum size effects.

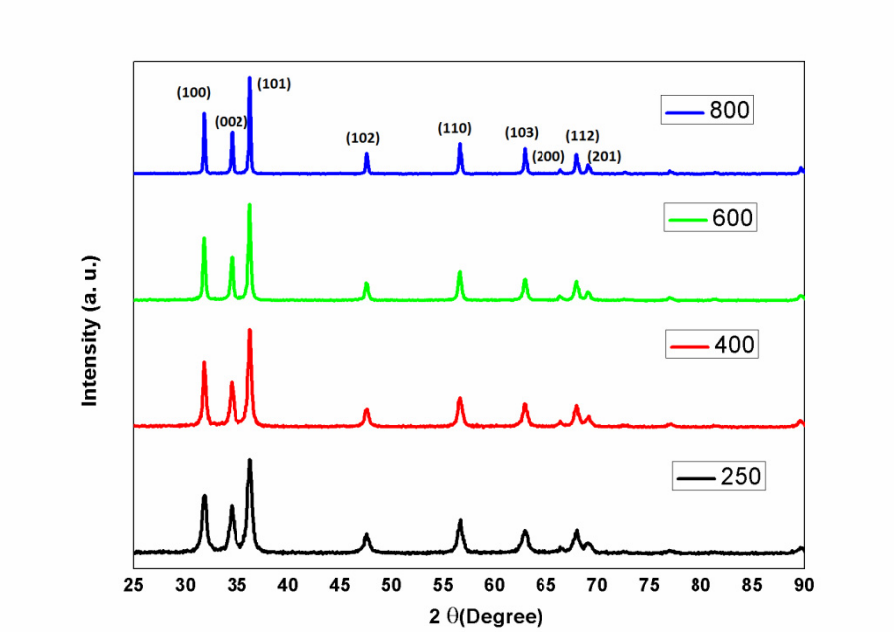

Figure 1: XRD patterns of the ZnO annealed at various temperatures.

Table 1: Lattice constants, particles size, strain and bond length as calculated from XRD data for various annealing temperatures.

Annealing temperature(˚C)	Lattice constant"c" (Å)	Lattice constant"a" (Å)	Particle Size (nm)	Strain (η)	Zn-O Bond Length (Å)
250	5.214	3.249	16.49	0.0014	1.978
400	5.214	3.254	21.73	0.0014	1.981
600	5.214	3.254	28.85	0.0014	1.981
800	5.207	3.254	40.40	0.000077	1.980

The quantum size effect decreases with increase in temperature, since the particle size increases. It is interesting to note that with increasing temperature, the lattice parameter 'c' decreases while the lattice parameter 'a' increases. This indicates that as we change T from 250 ˚ C to 800 ˚ C, the initial shape of the nanoparticles change. The change in the lattice parameters on increasing the temperature can be attributed to dispelling of local lattice disorders, vacancies of oxygen and vacancy clusters.

The size of the nanoparticles can be estimated by using the broadening of the peaks in the XRD pattern. The average size of the ZnO nanoparticles was calculated according to the standard Debye-Scherrer Formula, $D = \frac{k\lambda}{\beta \cos\theta}$ (2)

where D is the size of the particle, β is the full width at half maximum in radians, λ= 1.5418 Å is the X-ray wavelength, k= 0.90 is the Scherrer Constant for spherical particles and θ is the angle between the X-ray source and the detector. The results for the particle size D for different temperatures are shown in table 1. As can be seen, the size of the particles increases with temperature. Size effect is not the only source of peak broadening but can also be due to strain in the particles. The strain in the ZnO nanoparticles along the c-axis can be calculated using the formula[28],

$$\eta = \frac{(c - c_0)}{c_0} \tag{3}$$

Where c denotes the measured lattice parameter and c_0 is the unstrained lattice parameter for bulk ZnO [29]. The calculated value of the strain η for different annealing temperatures has been given in table 1. The values of the strain from table1 reveal that at T=800 ˚ C, the strain is substantially reduced and approaches towards the bulk value. This observation is consistent with our results for the lattice parameters which approaches the bulk value at T=800 ˚ C. The Zn-O bond length L can be evaluated using the expression [28],

$$L = \left[\frac{a^2}{3} + \left(\frac{1}{2} - u \right)^2 c^2 \right] \tag{4}$$

$$u = \frac{a^2}{3c^2} + 0.25, \tag{5}$$

The values obtained for the bond lengths are indicated in table 1. The known value of Zn-O bond length is 2.21 Å [30]. The small values obtained for our samples indicate the presence of structural defects like oxygen vacancies.We now estimate the band gap from the XRD data. The best XRD data are for peak (110) and it is therefore used for investigating the relation between the XRD- Particle size and the optical band gap. Based on the effective mass approximation and which has the same functional dependence as Brus equation, the following equation is used to determine the optical band gap (in eV) from the (110) peak [31],

$$E_g^{(110)} = 3.22 + \frac{0.896}{D} + \frac{2.86}{D^2} \tag{6}$$

The (110) peak is used if the particle shape is spherical. It does not contain any information about the size in the c-direction. The c-axis usually is the most energetically favorable. In order to estimate the optical band gap if the particles are elongated, the (103) peak is used, and the corresponding equation is [31],

$$E_g^{(103)} = 3.23 + \frac{1.64}{D} + \frac{0.441}{D^2} \tag{7}$$

The results from the peaks (110) and (103) are shown in table 2. The higher values of Eg at lower temperatures are attributed to “quantum size effects” [31]. Quantum confinement increases the band gap energy of ZnO. At lower temperature of T= 250 ˚C , the particle size is small and hence the quantum confinement effect is also comparatively large.

Table 2: Effect of annealing temperature on the calculated band gap.

Temp (˚C)	$Eg^{(110)}$ (eV)	$Eg^{(103)}$ (eV)
250	3.28	3.33
400	3.27	3.30
600	3.25	3.29
800	3.24	3.27

UV-Visibile Absorption Spectrum

Figure 2 shows the UV-vis Spectra of ZnO nanocolloid particles synthesized at different annealing temperatures. The samples (except for the one at 800˚C) exhibit strong absorption peaks in the range of ~ 360 nm to 380 nm, which is attributed to the electronic transition of electrons from valence band to conduction band. The exciton absorptions at 369 nm, 372 nm, and 376 nm at T= 250 ˚C, 400 ˚C and 600 ˚C respectively are blue shifted with respect to the bulk absorption peak at 388 nm . The sample annealed at T=800 ˚C shows very weak absorption at 403 nm, more than the band-gap wavelength of 388 nm. It is possible that at T=800 ˚C, the particle size is large and begins to agglomerate and form clusters in the solution. As a result, the material settles down on the bottom of the cuvette causing decrease in absorbance.

It is clear that the absorption peak systematically shifts to lower wavelengths with decreasing temperature (hence decreasing particle size). This pronounced and systematic shift is attributed to the quantum size effects. Thus the average particle size in a nanocolloid can be determined from the UV-Vis absorption spectra using the effective mass model [21]:

$$Eg = Eg^{bulk} + \frac{\hbar^2\pi^2\left(\frac{1}{m_e^*}+\frac{1}{m_h^*}\right)}{2r^2} - \frac{1.8e^2}{4\pi \in \in_0 r} - \frac{0.124e^4}{\hbar^2(4\pi \in \in_0 r)^2}\left(\frac{1}{m_e^*}+\frac{1}{m_h^*}\right) \quad (7)$$

Eg = Band gap energy determined from the UV-Vis Absorbance spectrum.

Eg^{bulk} =Bulk value of band gap energy = 5.126 x 10^{-19} J

r= Particle radius

m_e^* = effective mass of electron in the conduction band of ZnO.

m_h^* = effective mass of hole in the valence band of ZnO.

$\in_0$ = 8.854 x 10^{-12} $C^2N^{-1}m^{-2}$

$\in$ = relative permittivity of ZnO = 5.7

The band gap Eg = $\frac{\hbar c}{\lambda}$

The calculated particle size (2r) as the annealing temperature is increased as shown in table 3. As temperature increases, the peak absorbance wavelength becomes red shifted due to decreasing quantum confinement with increasing particle size.

Table 3: Effect of annealing temperature on particle size

Annealing temperature (˚C)	Peak absorbance wavelength (nm)	Particle size (nm)
250	369	3.93
400	372	4.15
600	376	4.41

Photoluminescence (Pl) Properties

Photoluminescence spectroscopy is an important tool to study the optical properties of semiconducting materials. Figure3 shows the photoluminescence spectra of ZnO nanoparticles at various annealing temperatures over the wavelength range 300-600 nm on irradiating at wavelength λ_{ex} = 323 nm *

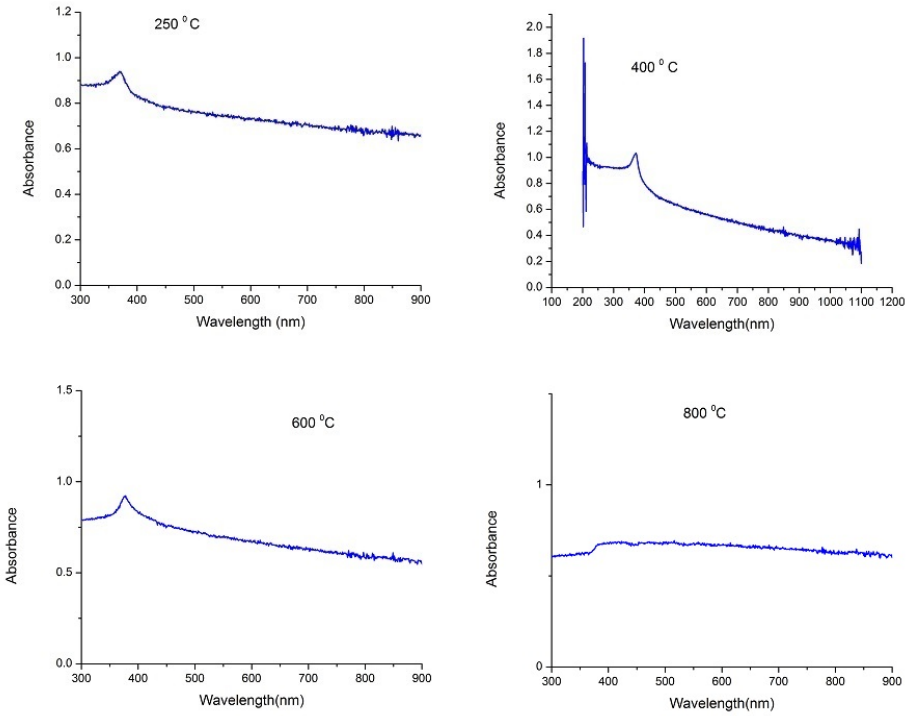

Figure 2: UV-Vis absorption spectra of ZnO nanoparticles are various annealed temperatures.

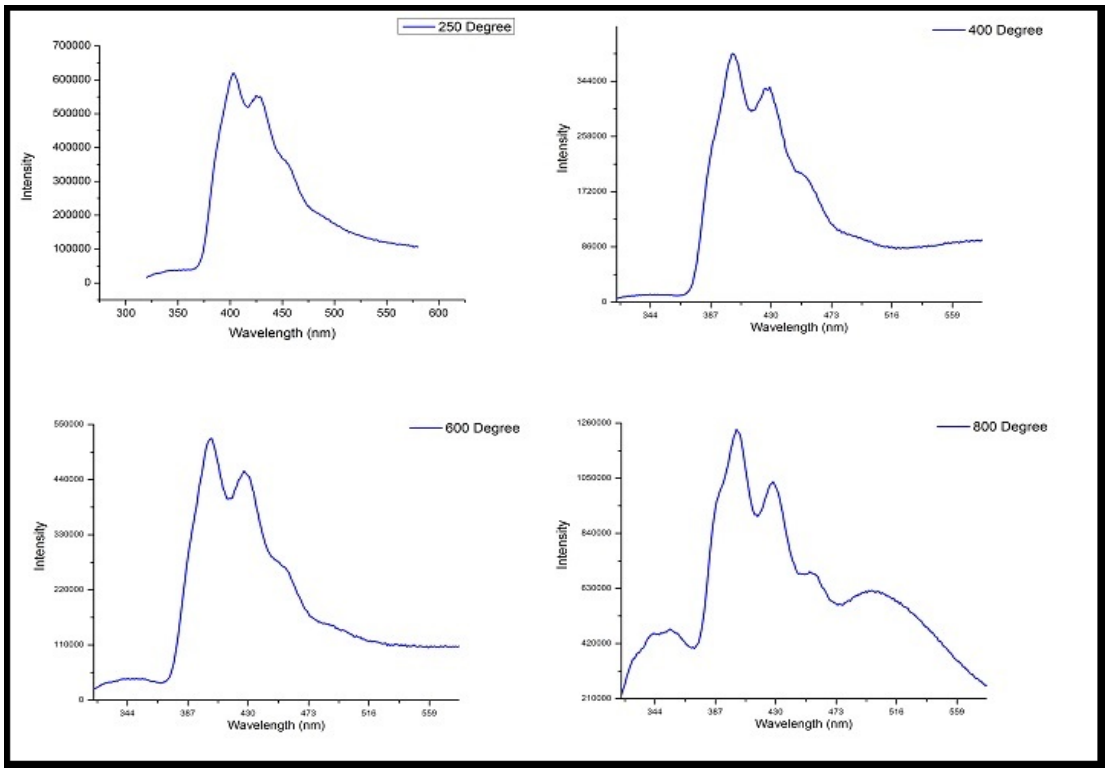

Figure 3: Photoluminescence spectra of ZnO nanoparticles at different annealing temperatures.

The PL spectra at T= 250, 400 and 600 ˚C shows peak in the violet region around 407 nm and two peaks in the blue region at around 426 and 455 nm. The violet emission is attributed to the transition from the Zn_i states (interstitial Zinc levels) to the valence band. The Zn_i levels are about 0.22 eV below the conduction band edge. The two blue peaks at 426 nm and 455 nm are attributed to the transitions from the extended Zn_i levels to the valence band. The extended Zn_i states are slightly below the simple Zn_i states and are formed during the annealing process. The PL spectrum at T= 800 ˚C has the usual peaks at about 404 nm, 429 nm and 455 nm. The blue peak at 455 nm is comparatively prominent for T = 800 ˚C sample. Interestingly two additional PL peaks are seen for T= 800 ˚C sample. One is at 355 nm and the other is at 499 nm. After High temperature annealing, the usual band edge emission in the UV band (355nm) and the deep level emission in the green band(499 nm) can be seen. The green emission originates from multiple defects. It is attributed to the transition from the near conduction band edge to the deep acceptor levels.

Tunneling Electron Microscopy (Tem)

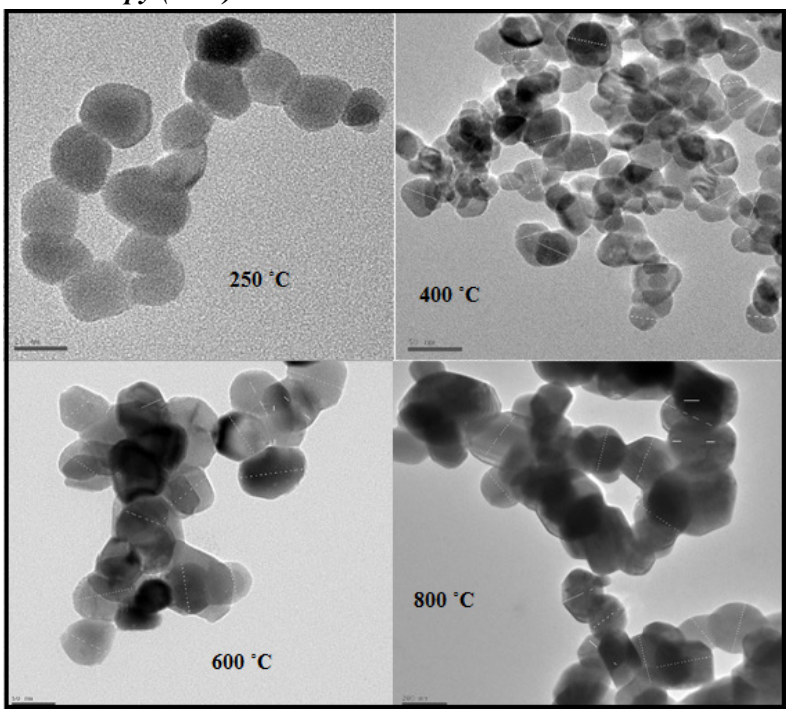

Figure 4: High resolution transmission electron microscopic pictures of ZnO nanoparticles at different annealing temperatures.

TEM micrographs of the ZnO nanoparticles annealed at different temperatures shown in Figure 4, reveals the nanostructures. The average grain size at different annealing temperatures approximately coincides with that found from XRD data. Interestingly at 800^{o}C, the TEM micrograph shows agglomeration.

Possible Anti-Bacterial Activity

Based upon the results reported in this manuscript and earlier studies [32], it can be assumed that with decreasing particle size the number of particles per unit volume increases resulting in increased surface area and hence inhibits the growth of bacteria. The increase in surface area determines the potential number of reactive groups on the particle surface, which are expected to show high anti-bacterial activity.

Conclusions

In this paper, we report on the effect of annealing temperature on the structure, morphological and optical properties of ZnO nanoparticles using chemical precipitation method at 200^{o}C, 400^{o}C, 600^{o}C and 800^{o}C. The XRD analysis revealed that the average size of the ZnO nanoparticles and the Zn-O bond length increased with increasing annealing temperature. As the particle size increased, the strain produced along the c-axis and the optical band gap decreased. The higher values of the optical band gap at lower temperatures are attributed to "quantum size effects". The UV-Vis absorption results confirmed that the particle size increases with annealing temperature. The Photoluminescence spectroscopy of ZnO nano-particles annealed at 800 ˚C revealed two additional peaks at 355 nm and the other is at 499 nm. TEM results showed agglomeration at 800 ˚C. We can conclude from our study that ZnO nano-particles annealed at low temperatures which have small particle size are best suited for anti-bacterial applications.

References

[1]. M. S. Tokumoto, V. Briois, C. V. Santilli, and S. H. Pulcinelli, *Journal of Sol-Gel Science and Technology*, 26(2003), 547–551.
[2]. P. Kumar, L. S. Panchakarla, S. V. Bhat, U. Maitra, K. S. Subrahmanyam, and C. N. R. Rao, *Nanotechnology*, 21(2010), 385701.
[3]. G. Thomas, *Nature*, 389(1997), 907–908.
[4]. M. Mazur, Electrochemistry Communications, 6 (2004) 400-403.
[5]. L. Feng, C. Zhang, G. Gao and D. Cui, Nanoscale Research Letters, 7:276 (2012) 1-10.
[6]. A. Pal, S. Shah and S. Devi, Colloids and Surfaces A Physicochemical and Engineering Aspects, 302 (2007) 483-487.
[7]. I. Singh, R. Kumar and B. I. Birajdar, *Journal of Environmental Chemical Engineering,* 5(2017) 2955–2963.
[8]. Y. Xie, R. Ye and H. Liu, Colloids and Surfaces A Physicochemical and Engineering Aspects, 279 (2006) 175-178.
[9]. V. Srikant and D.R. Clarke, *J. Appl. Phys*, 83 (1998), 5447- 5451.
[10]. X. Li and Y. Wang, J. Alloys Compd, 509 (2011) 5765–5768**.**
[11]. E. Pyne, G.P. Sahoo, K. Bhui, H. Bar, P. Sarkar, S. Samanta, A. Maity and A. Misra, Spectrochim. Acta, Part A , 93 (2012)100-105.
[12]. K. Venkatasubramanian and S. Sundaraj, *Chemical Science review letters*, 3 (2014), 40-44.
[13]. H. T. Ng, B. Chen, J. Li et al., *Applied Physics Letters*, 82(2003),2023–2025.
[14]. E. Topoglidis, A. E. G. Cass, B. O'Regan, and J. R. Durrant, *Journal of Electroanalytical Chemistry*, 517(2001),20–27.
[15]. P. Sharma, K. Sreenivas, and K. V. Rao, *Journal of Applied Physics*, 93(2003), 3963–3970.
[16]. P. V. Kamat, R. Huehn, and R. Nicolaescu, *Journal of Physical Chemistry B*, 106 (2002), 788–794.
[17]. W. Chen, Y.H. Lu, M. Wang, L. Kroner and H.J. Fecht, *J. Phys. Chem C,* 113(2009) 1320–1324.
[18]. H.Y. Yue, W.D. Fei, Z.J. Li and L.D. Wang, *J. Sol-Gel Sci. Technol*. 44(2007) 259–262.
[19]. A. K. Zak, M. E. Abrishami, W.H. Abd. Majid, R. Yousefi and S.M. Hosseini, *Ceramics International*, 37(2011),393-398.
[20]. T. D. Malevu and R.O. Ocaya, *Int. J. Electrochem. Sci.,* 10(2015),1752-1761.
[21]. S. Talam, S. R. Karumuri and N. Gunnam, doi:10.5402/2012/372505, 2012.
[22]. H. Kumar and R. Rani, *Int. Letts. Chem, Physics & Astronomy,* 14(2013), 26-36.
[23]. J. Yang, *Sensors*, 13(2013) 2719 -2734.

[24]. V. Ghafouri, A. Ebrahimzad and M. Shariati, Sci. Iran, 20 (2013) 1039–1048.
[25]. H.C. Wang, C.H. Liao, Y.L. Chueh, C.C. Lai, P.C. Chou and S.Y. Ting, *Optical Materials Express*,3 (2013), 295-306.
[26]. K.S. Hwang, Y.J. Lee and S. Hwangbo, *J Ceram Process Res*, 8 (2007) 305-311.
[27]. H.S. Chin and L.S. Chao, *J Nanomater*, 2013(2013) doi: 10.1155/2013/424953.
[28]. D. I. Rusu, G. G. Rusu and D. Luca, *Acta Phys. Polonica*, 119(2011), 850-856.
[29]. G.I. Rusu, M. Diciu, C. Pîrghie and E.M. Popa, *Appl. Surf. Sci*., 253(2007), 9500.
[30]. J. Mass, P. Bhattacharya and R. S. Katiyar, *Mater. Sci. Eng. B*, 103(2003), 9-15.
[31]. T. J. Jacobsson, "Synthesis and characterisation of ZnO nanoparticles. An experimental investigation of some of their size dependent quantum effects", PhD Thesis, Uppsala University, (2009).
[32]. N. Sharma, J. Kumar, S. Thakur, S. Sharma and V. Shrivastava, *Drug invention today*, 5(2013), 50-54.